AD-750 402

10.6 MICROMETER DETECTOR ARRAY

R. Lange, et al

AIL

AD750402

10.6 MICROMETER DETECTOR ARRAY

First Quarterly Report
(1 April 1972 to 1 August 1972)

October 1972

by

R. A. Lange, A. DiNardo, R. Augeri, and D. Yustein

AIL Report 0123-I-1
Prepared Under Contract N00014-72-C-0446
Project Code 2E90K21

for

Office of Naval Research
Washington, D. C.

Sponsored by

Advanced Research Projects Agency
ARPA Order No. 1806, Amendment No. 2/02-09-72

by

AIL, a division of Cutler-Hammer
Deer Park, New York 11729

The views and conclusions contained in this document are those of the authors and should not be interpreted as necessarily representing the official policies, either expressed or implied, of the Advanced Research Projects Agency or the U.S. Government.

D D C
RECEIVED
OCT 24 1972
B
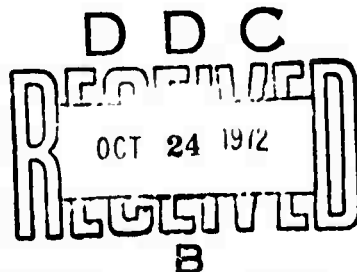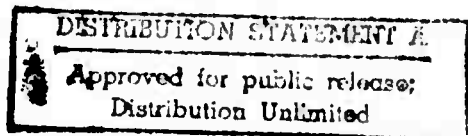
DOCUMENT CONTROL DATA - R & D

(Security classification of title, body of abstract and indexing annotation must be entered when the overall report is classified)

1. ORIGINATING ACTIVITY (Corporate author)	2a. REPORT SECURITY CLASSIFICATION
AIL, a division of Cutler-Hammer Deer Park, New York 11729	Unclassified
	2b. GROUP

3. REPORT TITLE

10.6 MICROMETER DETECTOR ARRAY

4. DESCRIPTIVE NOTES *(Type of report and inclusive dates)*
First Quarterly Report (1 April 1972 to 1 July 1972)

5. AUTHOR(S) *(First name, middle initial, last name)*

R. Lange, A. DiNardo, R. Augeri, and D. Yustein

6. REPORT DATE	7a. TOTAL NO. OF PAGES	7b. NO. OF REFS
October 1972	34	4

8a. CONTRACT OR GRANT NO.	9a. ORIGINATOR'S REPORT NUMBER(S)
N00014-72-C-0446	0123-I-1
b. PROJECT NO. ZE90K21	
c.	9b. OTHER REPORT NO(S) *(Any other numbers that may be assigned this report)*
d.	

10. DISTRIBUTION STATEMENT will follow.

11. SUPPLEMENTARY NOTES	12. SPONSORING MILITARY ACTIVITY
	Office of Naval Research Washington, D.C.

13. ABSTRACT

An optical design approach is presented with supporting optical field patterns calculated on a digital computer for a 10×10 element array of PV-HgCdTe elements operating in the heterodyne mixing mode at 10.6 micrometers. Mixed field patterns across the surface of the detector were calculated along with the far field diffraction pattern of the array showing the signal crossover levels between adjacent elements of the array.

Also discussed is an analysis of the power dissipation requirements of the photovoltaic mixers at 77 K. The local oscillator heating proved to be the highest with about 2 milliwatts dissipation required for near quantum noise limited operation at 1500 MHz. For a narrower bandwidth system of 150 MHz, the local power dissipation requirement may be reduced to several tenths of a milliwatt with the photodiode leakage current becoming the predominant power dissipating element.

DD FORM 1473
I NOV 65

KEY WORDS	LINK A		LINK B		LINK C	
	ROLE	WT	ROLE	WT	ROLE	WT
Heterodyne Imaging Array						
PV - HgCdTe						

ib

10.6 MICROMETER DETECTOR ARRAY

First Quarterly Report
(1 April 1972 to 1 August 1972)

October 1972

by

R. A. Lange, A. DiNardo, R. Augeri, and D. Yustein

for

Office of Naval Research
Washington, D. C.

Sponsored by

Advanced Research Projects Agency
ARPA Order No. 1806, Amendment No. 2/02-09-72

by

AIL, a division of Cutler-Hammer
Deer Park, New York 11729

iC

id

TABLE OF CONTENTS

LIST OF ILLUSTRATIONS

I. INTRODUCTION AND SUMMARY

This is the First Quarterly Technical Report under Contract N00014-72-C-0446, having as its objective the development of a technology required to build a large array of high-speed heterodyne receivers for 10.6-micrometer laser radiation. Toward this end the following areas will be examined:

- High density cabling techniques for low crosstalk and low thermal conductivity

- Thermal analysis for matrix arrays for 77 and 4.2 K for 150 and 1500 MHz bandwidth systems

- Thermal mock-up of cabling techniques used with the 77 K, 1500 MHz array

- Image plane dissection techniques for an array of 100 elements or larger made by batch processing techniques

- Testing of four HgCdTe photodiodes on a subassembly of the matrix array design used for the thermal mock-up

This program brings together the experience and techniques developed under Contract N00014-68-C-0273 for heterodyne arrays of 4.2 K Ge:Cu detectors and the experience of single element PV-HgCdTe receivers developed over the last several years.

II. IMAGING ARRAY AND ASSOCIATED OPTICS

A. TELESCOPE DESIGN FOR 77 K DETECTOR ARRAY

An optical system has been conceived which permits the construction of a 10 × 10 array of HgCdTe photovoltaic mixers with a frequency response of up to 1.5 GHz. The features of the design include:

- Ability of the array to be made up of individually mounted detector elements allowing implementation of the array concept with any number of detectors to prove feasibility, optimum choice of the array elements for a matched or more uniform response from the array, and allows replacement of damaged elements

- Low optical and electrical crosstalk between channels due to the relatively large spacing between detectors and the separate coaxial cable outputs

The optical approach chosen is shown in Figure 1 and is an extension of that which was developed under ONR Contract N00014-68-C-0273. The optical system is basically the same because an image is subdivided by an array of square lenses directing all the optical energy from one cell in the focal plane to the appropriate infrared mixer element. However, the HgCdTe photovoltaic detectors require a relatively large spacing between detectors to provide for mounting and cabling, and to ensure low electrical and optical crosstalk.

Because of this large spacing requirement, a matching lens was added to match the diffraction-limited spot in the primary focal plane of the telescope to a square image-dissection lens in the secondary focal plane. This matching lens effectively increases the f/number of the primary receiving optics to provide a diffraction limited disc that matches the image-dissection array. In this way, mixer center-to-center spacings of 7.5 mm (which would otherwise correspond to a telescope f/number of 300) can be achieved with a lower f/number requirement on the receiving optics.

In this configuration, the local oscillator is injected into the system between the matching lens and the image-dissection array. At the plane of the image-dissection array, the LO and signal are effectively plane waves with matched phase fronts. These two matched fields are then focused onto and mixed in the detector elements.
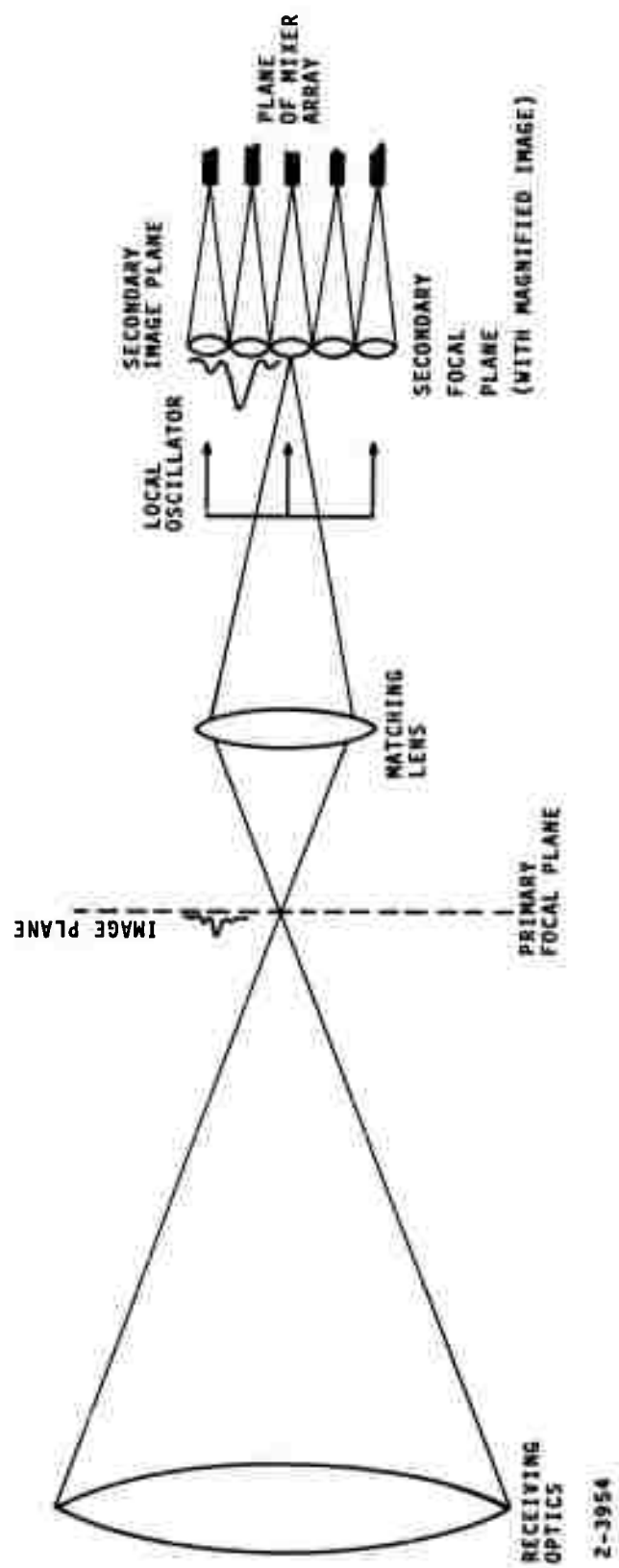
FIGURE 1. OPTICAL DIAGRAM OF IMAGING ARRAY

2-3954

B. ARRAY PATTERN SYNTHESIS

In order to analyze the behavior of the optical design presented in the previous section, it was necessary to mathematically formulate the optical train and obtain the fields of the local oscillator and signal that were mixed and detected in the focal plane of the image-dissection array. The optical pattern was found to be strongly affected by the reference phase front presented by the local oscillator. The mathematical formulation was programmed on a digital computer to give design information for optimizing the array patterns. The optical efficiencies and adjacent pattern cross-overs were obtained in this way.

First, consider the received signal that is focused by the telescope and the matching lens. For convenience we shall consider this lens combination as a single unit with the focal length and therefore the f/number of the telescope magnified by the ratio of the two focal lengths, such that,

$$f_1 = f_{telescope} \left(\frac{f_{telescope}}{f_{matching\ lens}} \right)$$

Then from reference 1, the electrical field distribution of the signal in the plane of the image-dissection lens array is given as:

$$I_0 = A2\pi a^2 \frac{J_1 \left\{ \frac{ka}{f_1} \left[(x + x')^2 + (y + y')^2 \right]^{1/2} \right\}}{\frac{ka}{f_1} \left[(x + x')^2 + (y + y')^2 \right]^{1/2}} \tag{1}$$

The terms of the expression are defined in Figure 2 which shows the coordinate system used for the array pattern synthesis. This expression describes a diffraction field of the form $J_1(x)/x$ in two dimensions with the center of the pattern displaced from the optical axis by a distance (x', y'). This represents the position of the center of a target that has moved from the optical axis of the telescope.

---

[1] Pace, F., Arams, F., Lange, R., Peyton, B., Sard, E., and Ramsey, J., "Advanced Capability Infrared Receiver System," First Semiannual Progress Report, AIL Report 3481-1-1, October 1968.
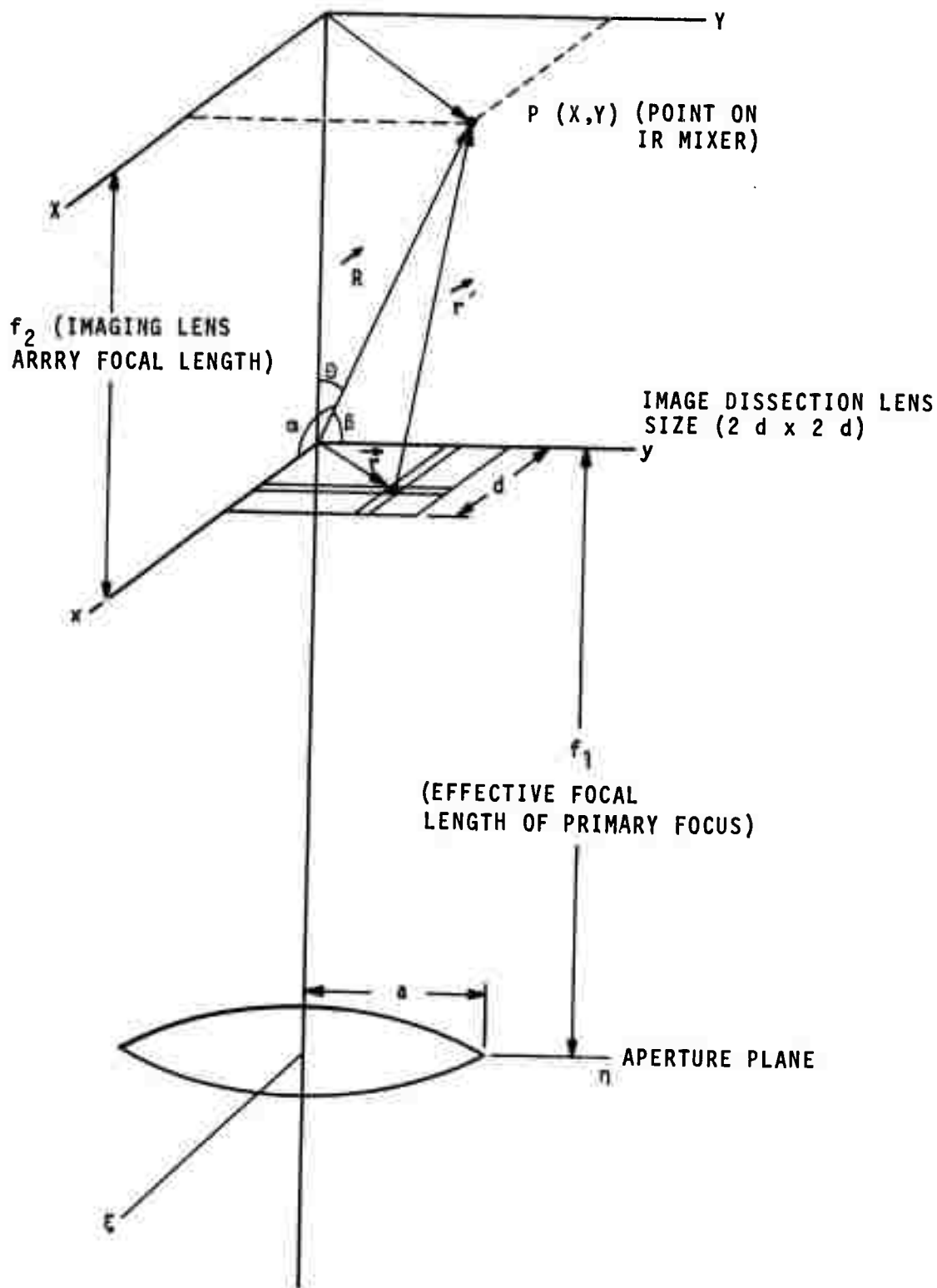
2-3955

FIGURE 2. COORDINATES FOR HETERODYNE RECEIVER BEAM
PATTERN ANALYSIS

5

The diffraction pattern formed in the focal plane of the image-dissection array due to the diffraction field incident upon the array can then be found from reference 2 as:

$$\overline{E}p_S(X, Y) = \int_{-d}^{d} \int_{-d}^{d} I_0(x, y) e^{ik(\alpha x + \beta y)} dxdy \qquad (2)$$

Substituting for I_0 in equation 2 and making a small angle approximation,

$$X = R\alpha = f_{2\alpha}$$

$$Y = R\beta = f_{2\beta}$$

we get:

$$\overline{E}p_S(X, Y) = 2\pi a^2 \int_{-d}^{d} \int_{-d}^{d} \frac{J_1\left\{\frac{ka}{f_1}\left[(x + x')^2 + (y + y')^2\right]^{1/2}\right\}}{\frac{ka}{f_1}\left[(x + x')^2 (y + y')^2\right]^{1/2}}$$

$$\cdot e^{i\frac{k}{f_2}(Xx + Yy)} dxdy \qquad (3)$$

where the integration is over that part of the $J_1(x)/x$ diffraction pattern that is incident upon the area of a particular image-dissection lens.

[2] Stroke, G., An Introduction to Coherent Optics and Holography, Academic Press, New York, p 22, 1966.

Consider now the local oscillator similarly focused by the image-dissection lens array and we get:

$$\overline{Ep}_{LO}(X, Y) = \int\limits_{-d}^{d} \int\limits_{-d}^{d} \underbrace{\frac{\sin mx}{mx} \cdot \frac{\sin my}{my} \cdot e^{\frac{ik}{f_2}(Xx + Yy)}}_{\substack{\text{local oscillator field} \\ \text{distribution over the} \\ \text{image-dissection lens}}} dxdy \qquad (4)$$

where $\overline{Ep}_{LO}(X, Y)$ is the electric field of the local oscillator wave in the focal plane of the image dissectors. The local oscillator was chosen to be a uniform plane wave so that $m = 0$ and $\sin mx/mx \cdot \sin my/my = 1$. Substituting these values into equation 4, we get:

$$\overline{Ep}_{LO}(X, Y) = \int\limits_{-d}^{d} \int\limits_{-d}^{d} e^{\frac{ik}{f_2}(Xx + Yy)} dxdy \qquad (5)$$

The time dependent forms of the signal and local oscillator fields can now be written as:

$$\overline{Ep}_S(X, Y, t) = C\, e^{-i(\omega t + kf_1)} \overline{Ep}_S(X, Y)$$

and

$$\overline{Ep}_{LO}(X, Y, t) = B\, e^{-i\omega_0 t} \overline{Ep}_{LO}(X, Y) \qquad (6)$$

where ω and ω_0 are the frequencies of the signal and local oscillator waves respectively.

The fields of the received signal and the local oscillator are now combined at the mixer by addition (assuming the polarization of the two components are aligned) and the intensity of the resultant computed.

$$I_i = < \left(E_{LO} + E_p \right)^2 > = \frac{1}{2T} \int_{-T}^{T} \left(E_{LO}^2 + E_p^2 + E_{LO} E_p^* + E_{LO}^* E_p \right) dt$$

(7)

The period of integration (2T) is taken very long compared to the period of the infrared frequency, but short compared to the period of the frequency difference introduced by the two cross terms. Therefore, the first two terms in the intergrand result in dc outputs from the mixer and are of no interest at this point. The two cross terms result in the intermediate IF signal. The mixer responds to the integrated intensity of the real part of the last two terms over its surface so that the mixer output is given by:

$$I_m = C' \left[\sin \ (\omega - \omega_o) \ t + kf_1 \right] \iint (Re) \ \overline{E}p_s \ (X, \ Y) \cdot \overline{E}p_{LO} \ (X, \ Y) \cdot dXdY$$

mixer
area

$$I_m = C'' \left\{ \sin \left[(\omega - \omega_o) \ t + kf_1 \right] \right\} \iint$$

$$\frac{J_1 \left\{ \frac{ka}{f_1} \left[(x + x')^2 + (y + y')^2 \right]^{1/2} \right\}}{\frac{ka}{f_1} \left[(x + x')^2 + (y + y')^2 \right]^{1/2}} \cdot e^{\frac{ik}{f_2} (Xx + Yy)} \quad dxdy$$

(8)

8

In equation 8, the argument of the sine term is made up of two parts. The first part is the time varying component that produces the IF signal. The second part is a fixed phase that can be dropped with no loss of generality.

C.   COMPUTER GENERATED ARRAY PATTERNS

In equation 8, the integral (I_m) which gives the IF signal output from a mixer element was computed to give the far field patterns for several combinations of LO and signal fields. Three dimensional plots of the mixed signal output over the detector surface were also computed for several angles of arrival of the signal with respect to one of the image-dissection lenses.

Figure 3 shows the value of I_m evaluated at 100 points across the surface of the mixer element. Each of the 100-unit areas was treated as a separate mixer and the integral I_m was evaluated at each with their sum representing the IF signal output of the mixer.

The parameters chosen were an f/400 telescope, a square $(1.1 \times 1.1$ cm) image-dissection lens f/3.8, and a plane wave local oscillator incident upon the image-dissection lens. The f/400 telescope approximately matches the diffraction-limited spot of the telescope to the square image-dissection lens rejecting most of the out-of-phase side lobe energy for the on-axis case. Figure 4 shows both the signal and local oscillator fields focused on the mixer. The product of these two fields yields the plot shown in Figure 3. As can be seen at the mixer, the signal field $(J_1(x)/x)$ approximately matches the size of the detector while the local oscillator field $(\sin x/x)$ is considerably narrower. This difference in the diameters of the signal and local oscillator spots is due to the different amplitude distributions across the image-dissection lenses. The signal spot is assumed to be centered on the image-dissection lens and has little or no energy at the edges of the lens and therefore its effect at the detector is as if the lens had a higher effective f/number. Since the diffraction limited spot size depends directly on f/number, we obtain a signal spot size larger than that of the local oscillator which has a uniform intensity distribution across the image-dissection lens aperture.

PLANE WAVE LO

$f_1/400$

$f_2/3.8$

SIGNAL AIRY DISK
MATCHED TO IMAGE
DISSECTION LENS
AND CENTERED

DISSECTION LENS (1.1 x 1.1 cm)

2-3956
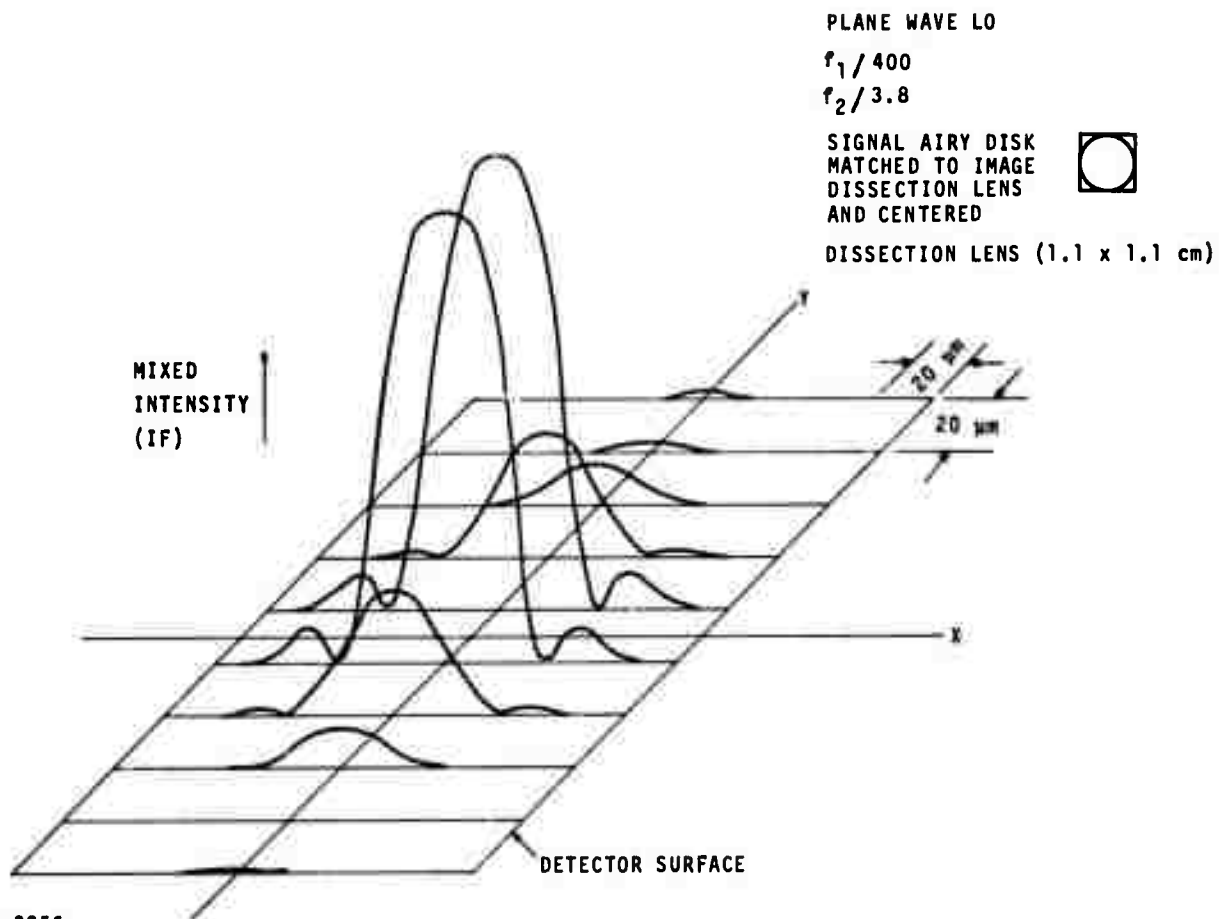
FIGURE 3.   MIXED INTENSITY AT DETECTOR SURFACE FOR PLANE
WAVE LO, $f_1/400$ AND SIGNAL CENTERED

10

LO FIELD
$\left(\dfrac{SIN X}{X}\right)$

FIELD E_{LO}
E_{SIGNAL}

SIGNAL FIELD

PLANE WAVE LO
$f_1/400$
$f_2/3.8$

SIGNAL AIRY DISK MATCHED
TO IMAGE DISSECTION LENS
AND CENTERED
DISSECTION LENS (1.1 x 1.1 cm)

Y

X

DETECTOR SURFACE

2-3957

FIGURE 4.   LOCAL OSCILLATOR AND SIGNAL FIELD AT
DETECTOR SURFACE

11

This combination of parameters introduces an inefficiency in that the phases of the signal and local oscillator are not matched across the surface of the mixer. Over the area of the LO airy disc, the signal and LO are both in phase and contribute to the IF signal output. The first side lobe of the LO also falls upon the detector surface but it is 180 degrees out of phase with the central field of the signal. The result is that the product of the two fields in this region is negative and subtracts from the IF signal output degrading overall receiver sensitivity. This degradation can be reduced by reducing the size of the detector or increasing the image-dissection lens f/number. The detector can then be matched to the size of the mixer airy disc rejecting most of the out-of-phase mixed signal.

In order to determine the crossover levels between elements of the array, the signal airy disc was positioned at the edge of the image-dissection lens with half of the airy disc energy falling on a single image-dissection lens. Figure 5 shows the mixed signal across the mixer face for this case with the same f/numbers and plane wave LO as Figure 3. If the detector was reduced in size to more effectively match the on-axis case, it would reduce the sensitivity at the crossover point. The reason for this is that the second ring of the diffraction pattern beyond the airy disc will no longer fall upon the mixer. This ring is in phase with the central field and has a significant amplitude. Therefore, rejection of this ring loses signal power causing a loss of sensitivity.

The second case to be examined has the same signal conditions $f_1/400$, $f_2/3.8$, and image-dissection lens (1.1×1.1 cm), but the local oscillator field across the image lens was changed as follows. An amplitude taper was applied to the local oscillator making it similar to the gaussian shaped signal field. This has the effect of matching the focused fields of the local oscillator and signal over the mixer surface such that the energy in the airy disc and the side lobes is additive to the IF signal. For this case it is advantageous to collect all of the IF signal energy by increasing the mixer size. Figures 6 and 7 show the mixed field across the mixer surface for the on-axis and edge case. It can be seen that the IF signal airy disc is now larger and better matches the detector size.

The third case is for a plane wave local oscillator, with all parameters the same as the first case except for a larger f/number telescope ($f_1/800$). This case is closer to that of a coherent heterodyne monopulse receiver where the signal airy disc is matched in size to a 2×2 square array of image-dissection lenses. This case has higher crossover levels and it is anticipated that this will not be an effective configuration for obtaining the best image resolution for a fixed number of array elements. It is,

PLANE WAVE LO

$f_1/400$

$f_2/3.8$

SIGNAL AIRY DISK MATCHED
TO IMAGE DISSECTION LENS AND
CENTERED ON EDGE

DISSECTION LENS (1.1 x 1.1 cm)

MIXED
INTENSITY
(IF)

Y

X

DETECTOR SURFACE

2-3958

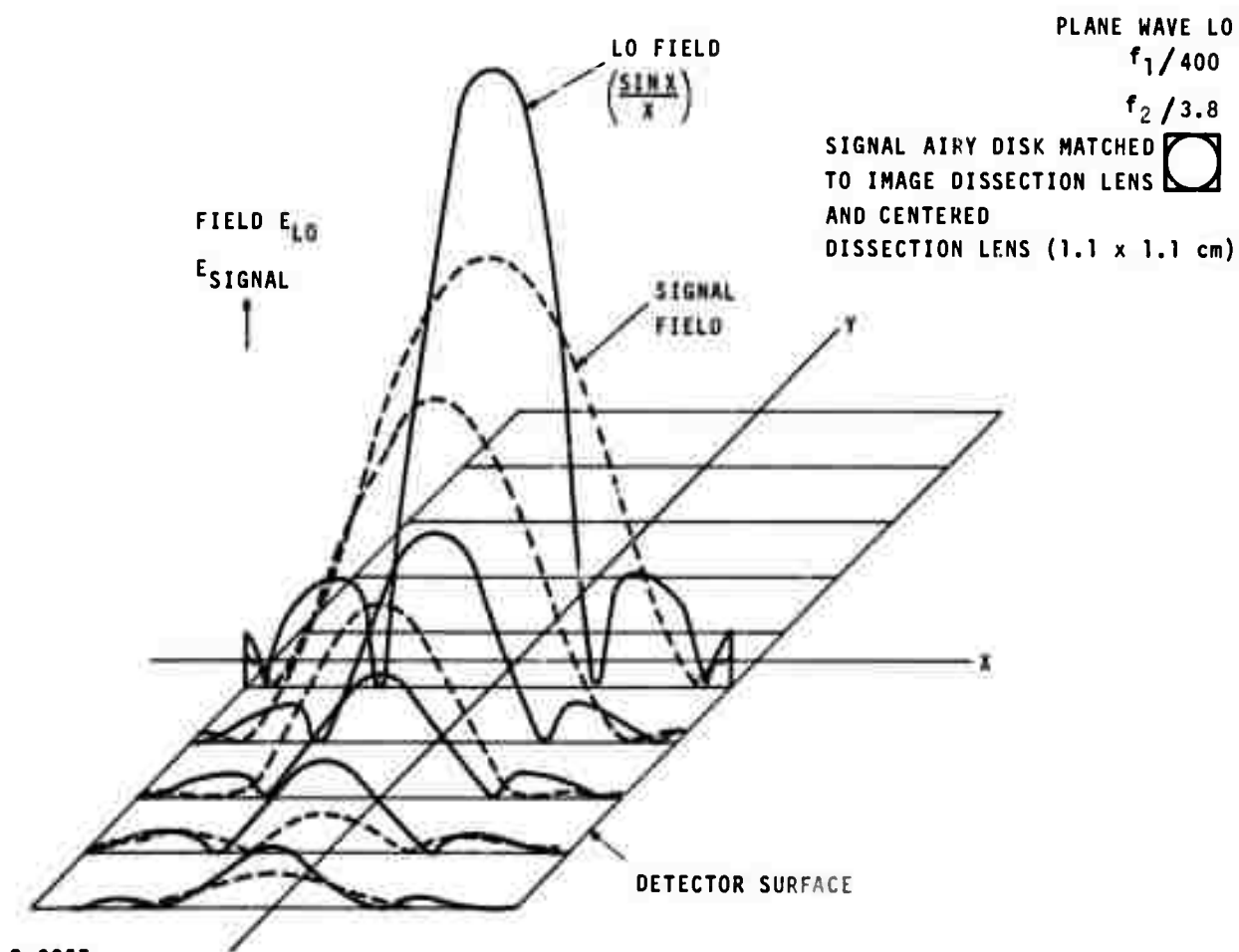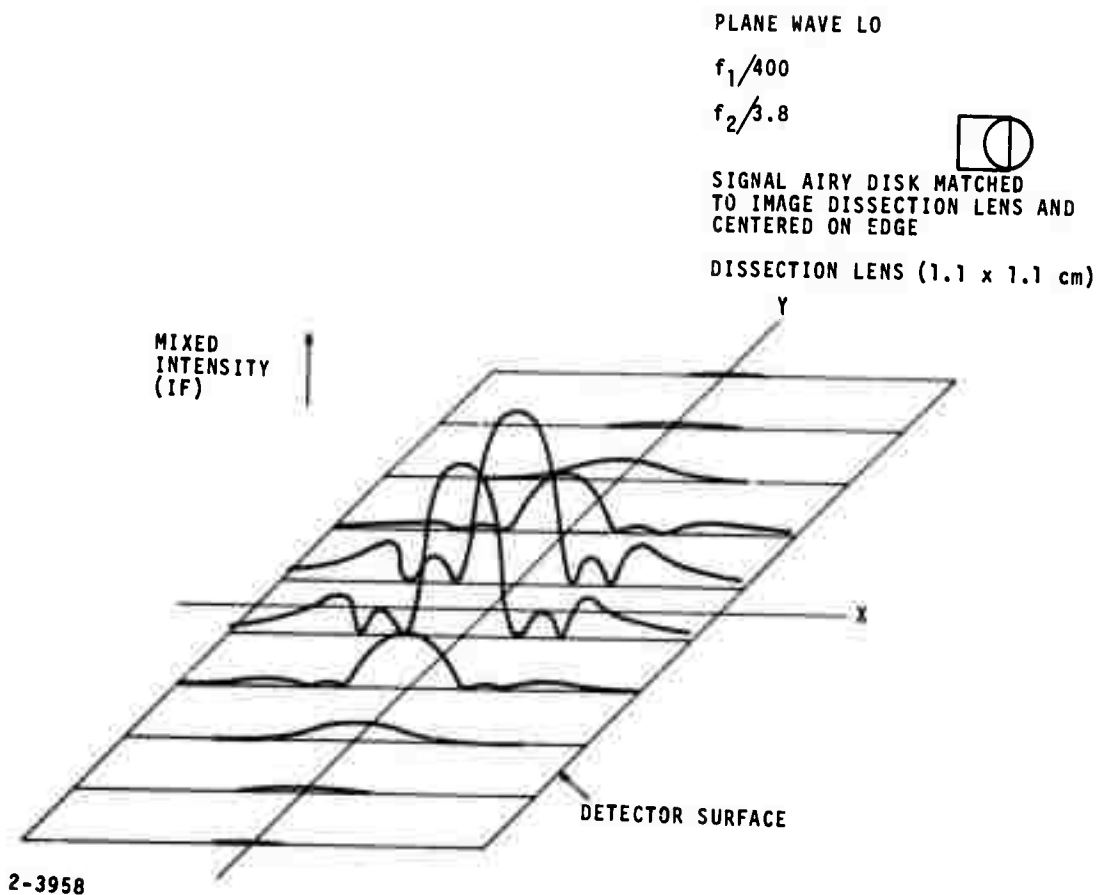FIGURE 5.   MIXED INTENSITY AT DETECTOR SURFACE FOR PLANE
WAVE LO, $f_1/400$ AND SIGNAL ON EDGE

13

FIGURE 6.   MIXED INTENSITY AT DETECTOR SURFACE FOR TAPERED LO, $f_1/400$ AND SIGNAL CENTERED
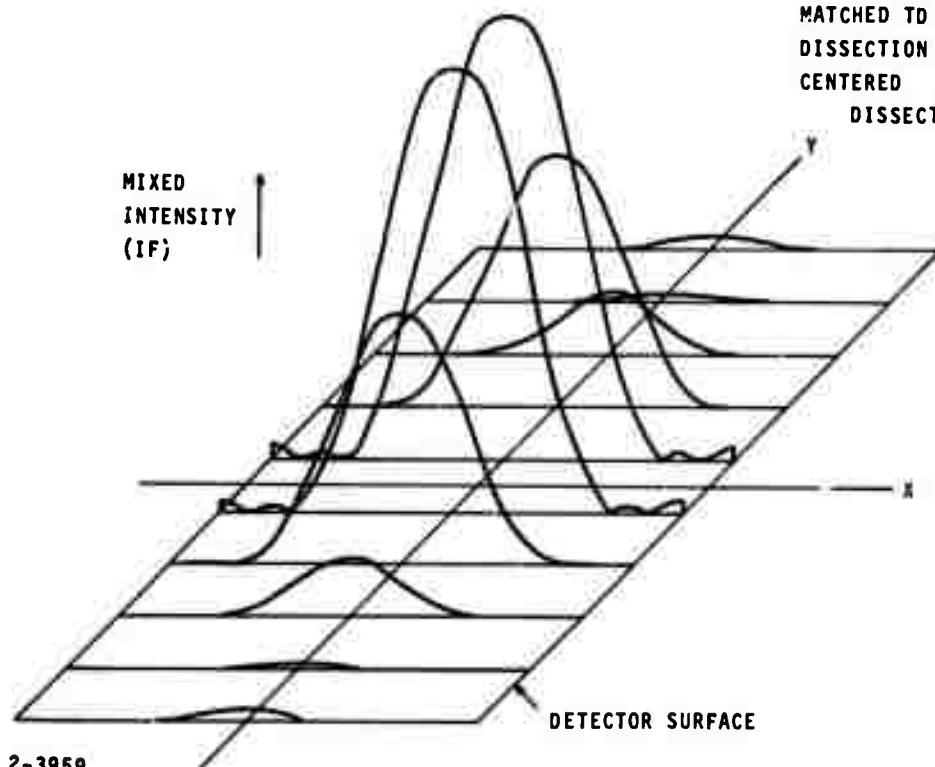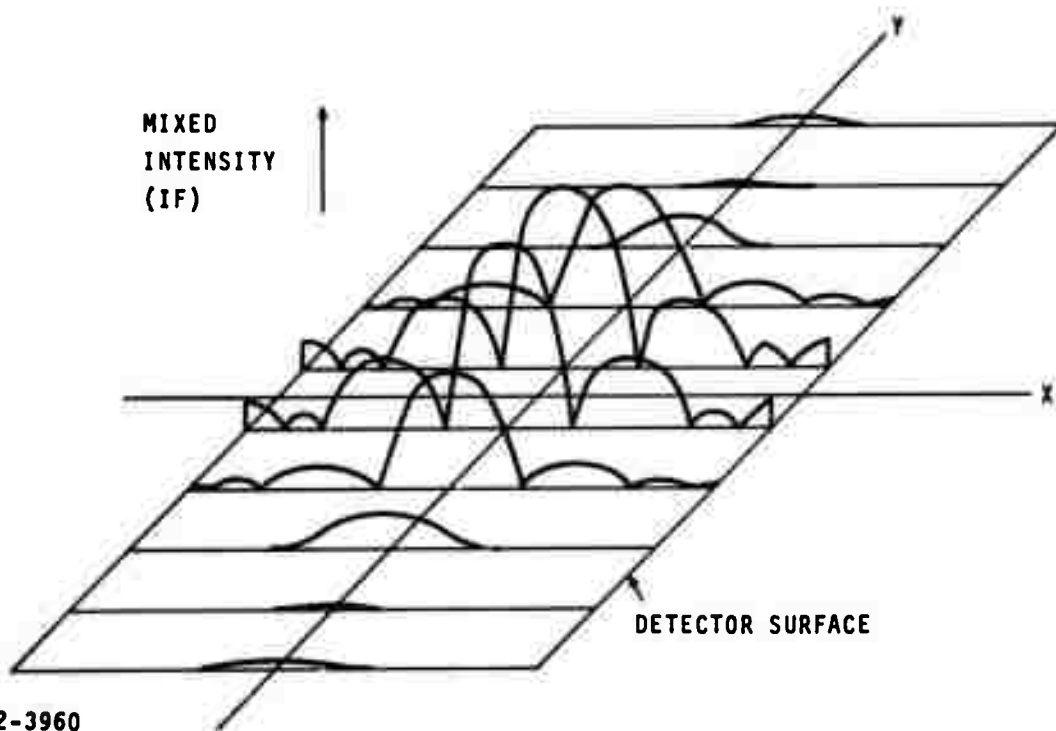
TAPERED LO
$f_1/400$
$f_2/3.8$

SIGNAL AIRY DISK MATCHED
TO IMAGE DISSECTION LENS
AND CENTERED ON EDGE
DISSECTION LENS (1.1 x 1.1 cm)

MIXED
INTENSITY
(IF)

Y

X

DETECTOR SURFACE

2-3960

FIGURE 7. MIXED INTENSITY AT DETECTOR SURFACE FOR TAPERED LO, $f_1/400$ AND SIGNAL CENTERED ON EDGE

however, another instructive case which shows a closer match of the LO and signal field across the detector with little out-of-phase IF contribution. This case has been measured in the laboratory and data is shown in Figure 2-11 of reference 1. This data agrees very closely with Figures 8, 9, and 10 and also shows very clean mixed IF patterns in the focal plane of an image-dissection lens array even with the signal airy disc centered on the edge of a dissection lens.

The far-field patterns for the three cases are shown plotted in Figure 11. This plot shows the integrated mixer outputs versus a normalized array element spacing. The crossovers are;

Local Oscillator	Telescope f/number	Edge Crossover	Corner Crossover
Plane Wave	400	- 4.3 dB	-8.1 dB
Plane Wave	800	- 2.2 dB	-4.8 dB
Tapered	400	-10.7 dB	----

From this correspondence between the telescope f/number and the crossover level, the optimum optical system can be obtained for use with a given array element spacing. This optimum crossover level, however, must still be obtained from a study of image quality for a finite number of individual resolution cells. For the purposes of proceeding with this program, this can be studied later since the only change needed to reoptimize would be the telescope f/number.
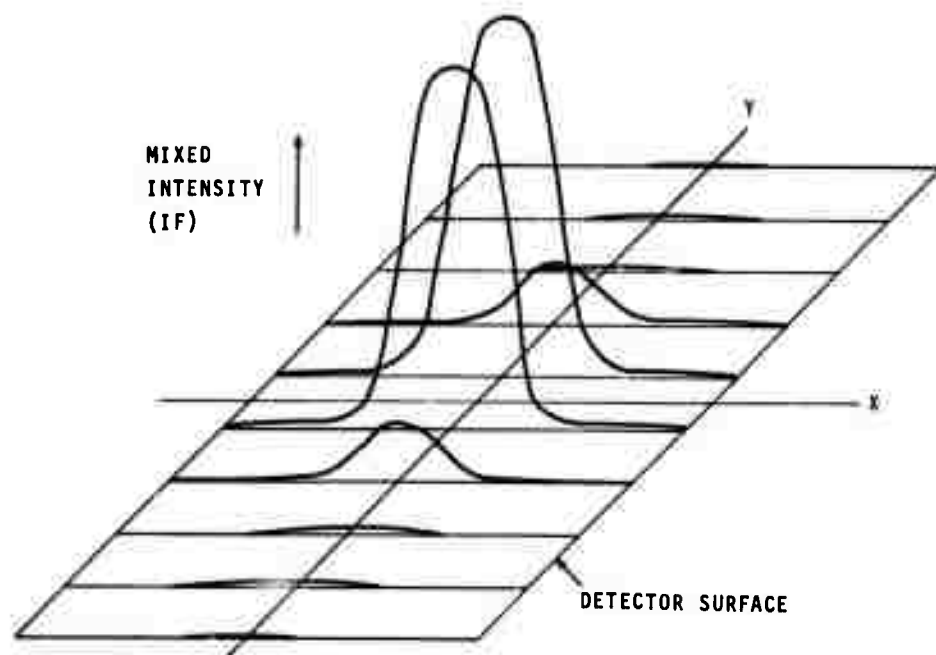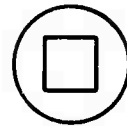
FIGURE 8. MIXED INTENSITY AT DETECTOR SURFACE FOR PLANE WAVE LO, $f_1/800$ AND SIGNAL CENTERED

TAPERED LO
$f_1/400$
$f_2/3.8$

SIGNAL AIRY DISK
MATCHED TO IMAGE
DISSECTION LENS AND
CENTERED ON EDGE
DISSECTION LENS (1.1 x 1.1 cm)

MIXED
INTENSITY
(IF)

DETECTOR SURFACE

2-3962
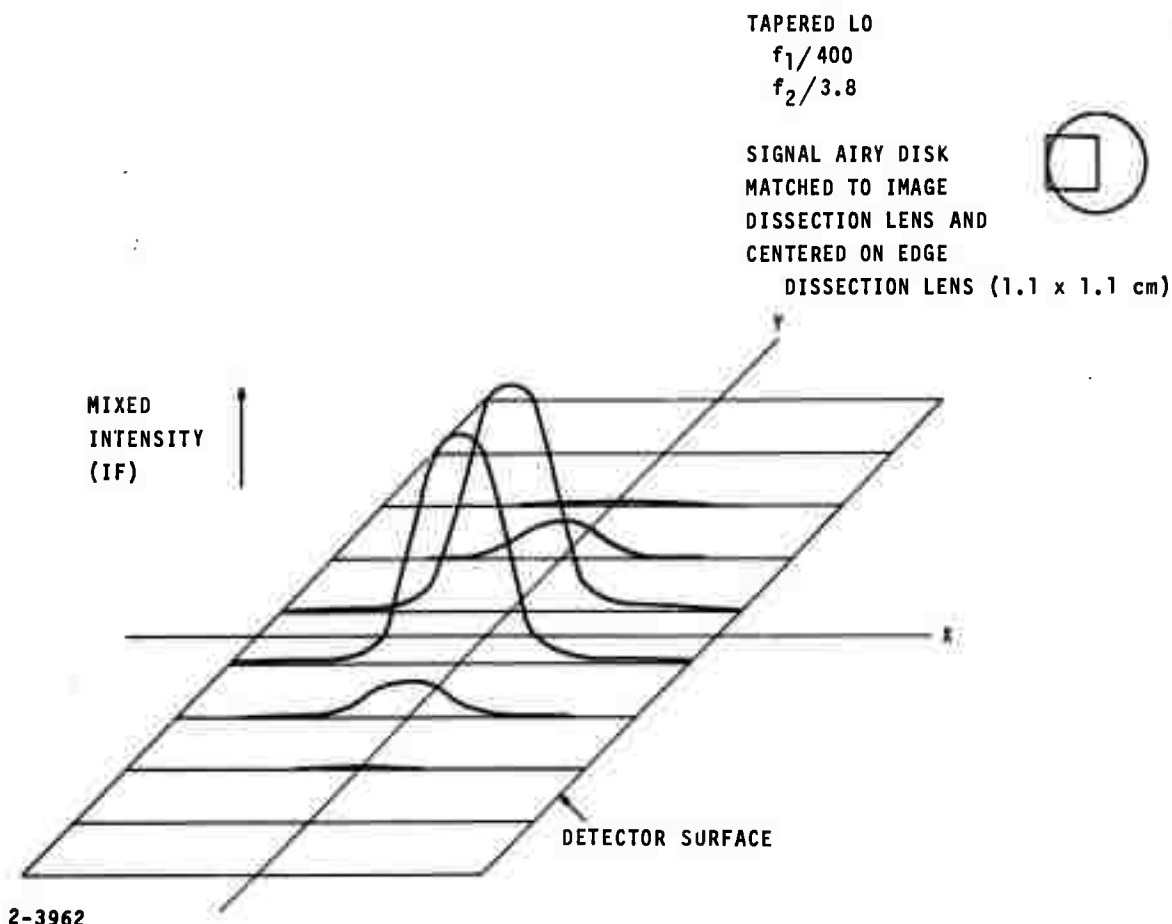
FIGURE 9.   MIXED INTENSITY AT DETECTOR SURFACE FOR PLANE
WAVE LO, $f_1/800$ AND SIGNAL CENTERED ON EDGE

18

PLANE WAVE LO

$f_1/800$

$f_2/3.8$

SIGNAL AIRY DISK
CENTERED ON EDGE
DISSECTION LENS (1.1 x 1.1 cm)

MIXED
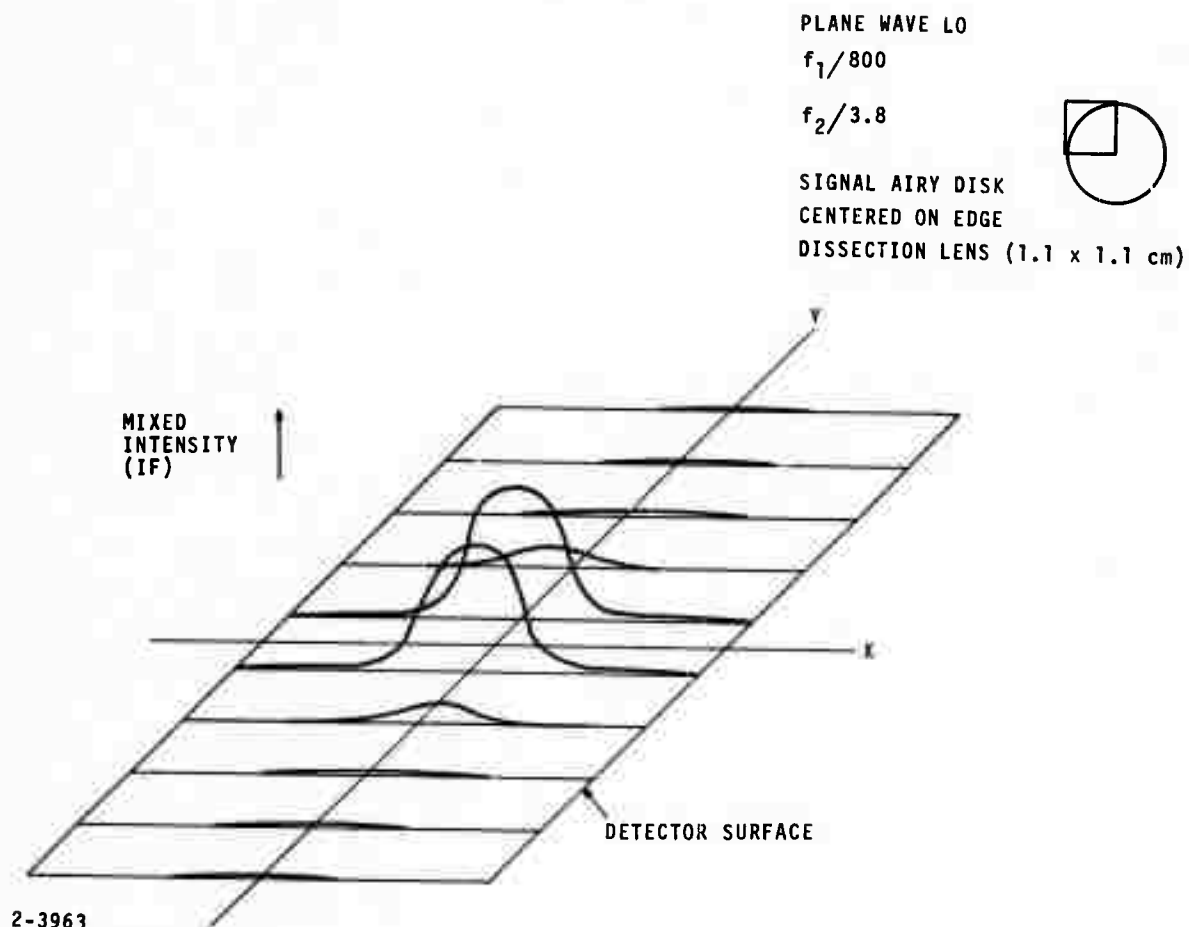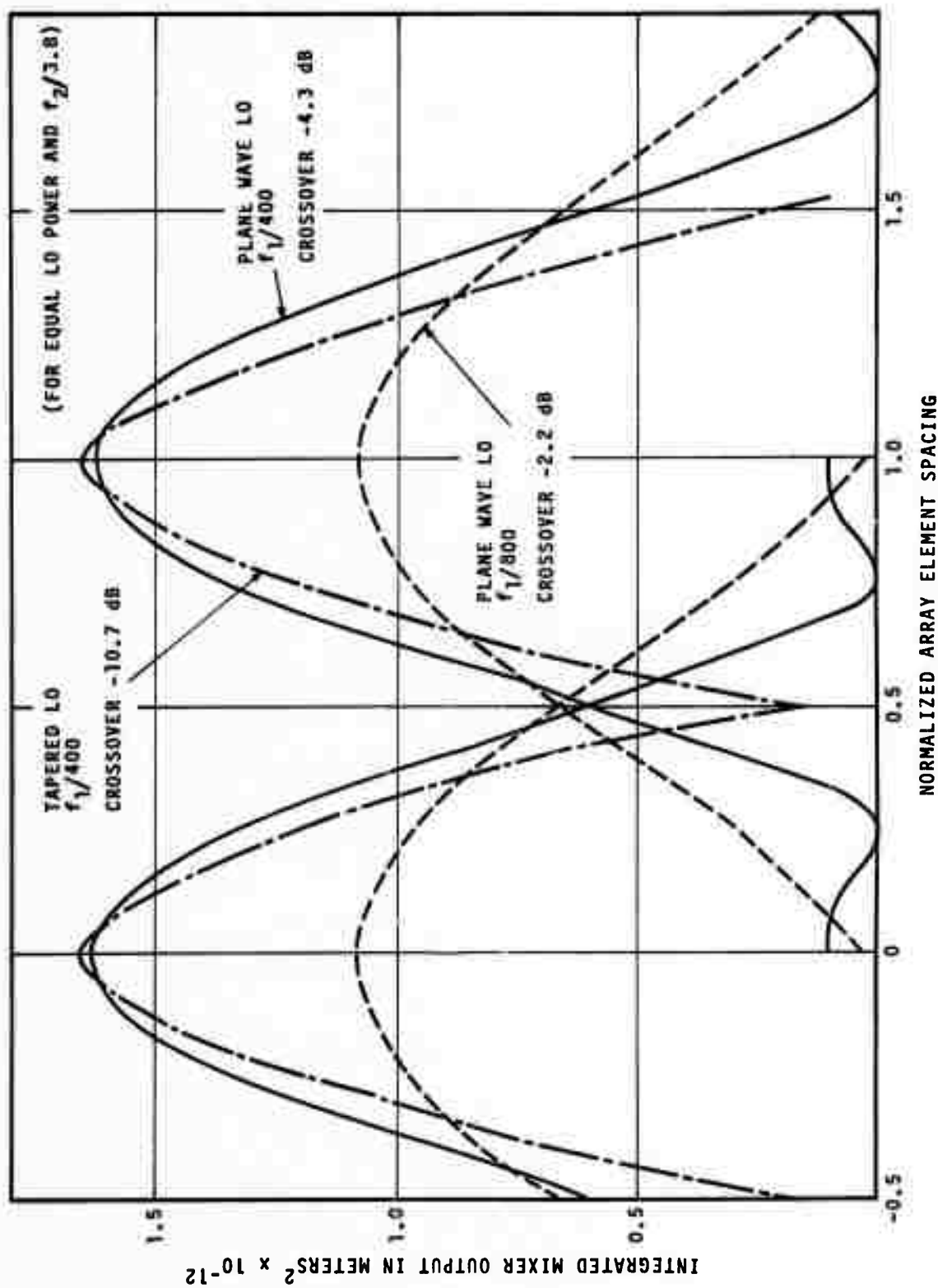INTENSITY
(IF)

DETECTOR SURFACE

2-3963

FIGURE 10. MIXED INTENSITY AT DETECTOR SURFACE FOR PLANE
WAVE LO, $f_1/800$ AND SIGNAL CENTERED ON CORNER

19

FIGURE 11. FAR FIELD ARRAY PATTERN FOR COMBINATION OF LO
AND SIGNAL ILLUMINATIONS

2-3964

20

III. POWER REQUIREMENTS FOR PV-HgCdTe PHOTOMIXERS

For efficient and stable operation of PV-HgCdTe photodiodes, they must be cooled to the neighborhood of 77 K. In order to maintain the mixers at this temperature, the cooler must be capable of handling the power absorbed through both the infrared local oscillator and the dc bias. The local oscillator and dc bias power requirements can be deduced from the mixer design equations presented in the following sections.

A. LASER LOCAL OSCILLATOR POWER REQUIREMENTS

It has been shown (reference 3) that for a PV-HgCdTe photo-mixer operating in the flat portion of its frequency response $(f/f_c << 1)$, quantum-noise-limited heterodyne operation is obtained when

$$I_o >> \frac{2k \, (T_m + T_{IF}') \, G_D}{q} \tag{9}$$

or

$$P_{LO} >> \frac{2k \, (T_m + T_{IF}') \, G_D \, h\nu}{q^2 \, \eta} \tag{10}$$

where

$\quad I_o \quad =$ dc photocurrent induced by the laser LO

$\quad k \quad =$ Boltzmann's constant

$\quad T_m \quad =$ physical temperature of the photomixer

$\quad T_{IF} \quad =$ effective input noise temperature of the IF preamplifier which is a function of its source conductance

----

[3] Peyton, B., DiNardo, A., Kanischak, G., Arams, F., Lange, R., and Sard, E., "High-Sensitivity Receiver for Infrared Laser Communications," IEEE J. Quantum Electronics, Vol. QE-8 No. 2, p 252-262, February 1972.

G_D = small-signal shunt conductance of the photomixer

q = electronic charge

h = Planck's constant

ν = infrared frequency

η = photomixer quantum efficiency

When the terms on the left and right side of equations 9 or 10 are equal, the thermal noise of infrared mixer and IF amplifier degrades the receiver sensitivity by 3 dB.

Calculated and measured data on 10.6 micrometer heterodyne receivers at AIL (reference 3) indicate that a properly designed heterodyne receiver can exhibit quantum-noise-limited operation for approximately 1 to 2 mW of incident laser LO power illuminating the PV-HgCdTe photomixer. Since photo-induced shot-noise must overcome the thermal noise of the photomixer and IF preamplifier, it is important to select a preamplifier which allows maximum transfer of shot noise so that the ratio of shot to thermal noise is maximized.

The measured receiver NEP as a function of incident LO power at an IF of 30 MHz is shown in Figure 12 for a PV-HgCdTe photomixer. In order to achieve quantum noise limited operation, it was necessary to operate with approximately 1.5 mW of local oscillator power incident upon the mixer. Photo-induced shot-noise exceeded the thermal noise for these values of LO power ensuring quantum-noise-limited operation and optimum receiver sensitivity.

By using the PV mixer design equation from reference 3, we can obtain curves of the receiver NEP versus local oscillator power for typical values of mixer parameters and IF frequency. The equation for NEP is:

$$NEP = \frac{h\nu B}{\eta}\left\{1 + \frac{2k(T_m + T'_{IF})h\nu}{q^2\eta P_{LO}}\left[G_D(1 + R_s G_D) + \omega^2 R_s C_D^2\right]\right\}$$

(11)
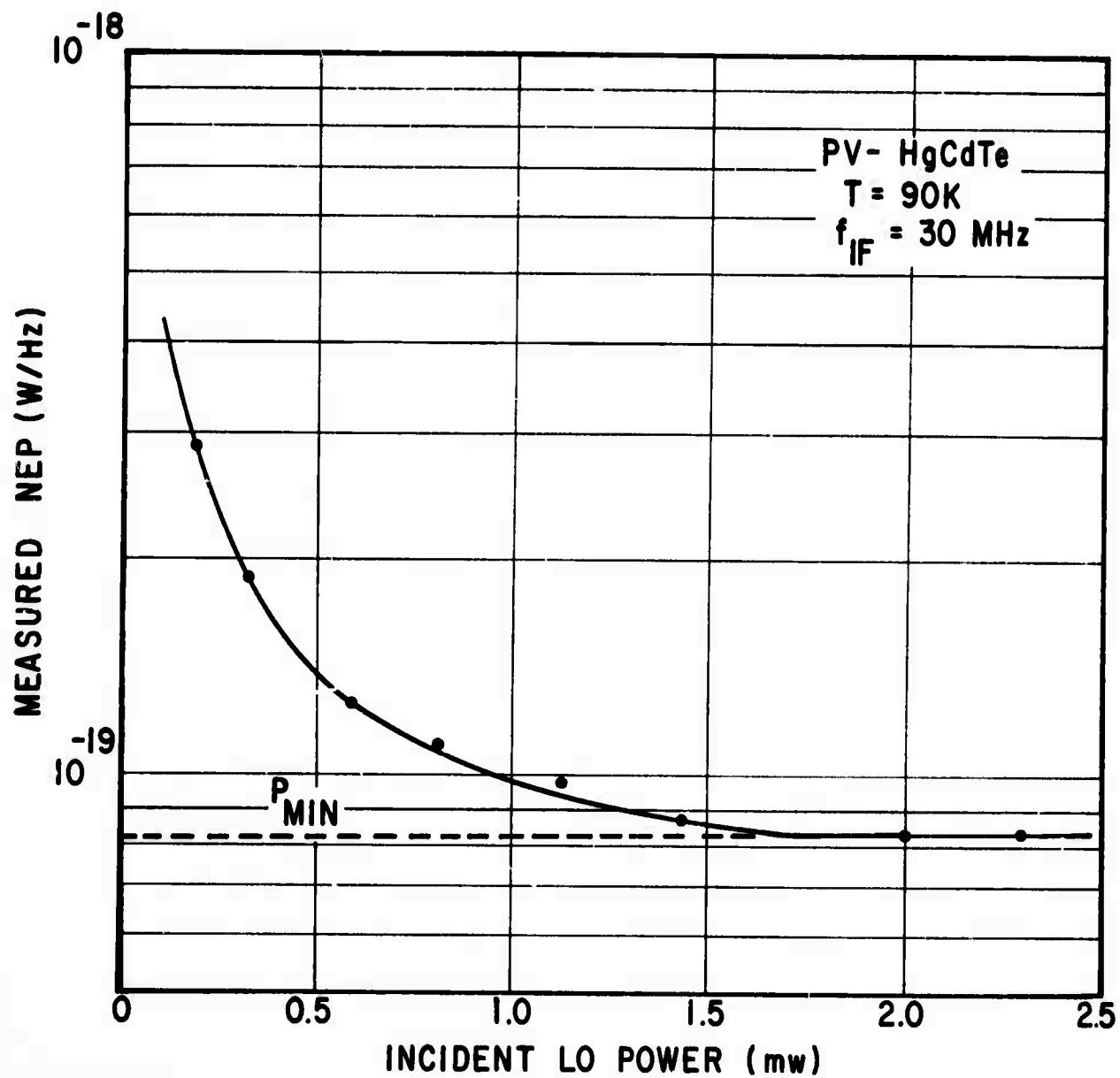
FIGURE 12.   MEASURED RECEIVER NEP AS A FUNCTION OF
OSCILLATOR POWER

V71-1253R2

23

where

$$T_{IF} = 293 \left[NF \left\{ 1 + \left[\frac{1}{2} \left(\frac{1}{50\,G'_{out}} + 50\,G'_{out} \right) - 1 \right] \right\} - 1 \right]$$

P_{LO} = local oscillator power

B = IF bandwidth

R_s = series resistance of diode

C_D = junction shunt capacitance

ω = IF

NF = noise figure of IF amplifier

G'_{out} = mixer output conductance

The terms of interest for obtaining the local oscillator power requirements are η, NF, G_D, R_s, and C_D. NF is the noise figure of the IF preamplifier which must be minimized to obtain a low effective input noise temperature of the IF amplifier. This, however, is limited by the state of the art of wideband IF preamplifiers and has a value which varies with the instantaneous IF bandwidth requirements of a particular system. We can assign typical values for the noise figure of 5.0 dB for a 1500 MHz and 2.5 dB for a 150 MHz bandwidth IF preamplifier. The remaining parameters are constants for a particular PV-HgCdTe photomixer. From reference 4 we can obtain the typical values of these parameters for high cutoff frequency PV-HgCdTe mixers as follows:

$$\eta = 25\%$$

$$G_D = 10^{-3} \text{ MHz}$$

$$R_s = 10 \text{ ohms}$$

$$C_D = 8 \text{ pf.}$$

---

[4] Vérié, C., and Sirieix, M., "Gigahertz Cutoff Frequency Capabilities of CdHgTe Photovoltaic Detectors at 10.6 μ," IEEE J. Quantum Electronics, Vol. QE-8 No. 2, p 180-184, February 1972.

Using these values and the 1500 MHz amplifier noise figure of 5 dB we can predict the NEP of the wideband mixer-preamplifier combination as a function of local oscillator power and IF frequency. There are, however, several partially compensating errors which were assumed in this analysis. The first is that the mixer capacitance is assumed to be a constant. This is an error since, as the detector is reverse-biased, the capacitance decreases thereby yielding a higher cutoff frequency detector with better NEP at the higher frequencies. The second assumption is the case of high quantum efficiency detectors which assumes that the detector is capable of producing as much photo-induced current, I_o, as is predicted by the local oscillator power and equation 12,

$$I_o = \frac{\eta q}{h\nu} P_{LO} , \tag{12}$$

There is a saturation effect which occurs at high photo-induced current corresponding to a decrease of quantum efficiency and accordingly degraded NEP.

The analysis is not capable of dealing with these two factors in that they vary greatly from detector to detector. However, since they are partially self-compensating, we use these assumptions to obtain a close approximation to the actual variation of system NEP with local oscillator power for a reasonable range of mixer parameters.

Figures 13 through 16 are a set of parametric curves obtained from equation 11 showing the NEP variation with local oscillator power for various combinations of R_s, G_D, η, and C_D evaluated at 150 MHz and 1500 MHz. A careful examination of these curves will indicate that:

- For mixers operating at 150 MHz bandwidth, the primary consideration for achieving near 10^{-19} w/Hz sensitivity is quantum efficiency. For mixers with quantum efficiencies greater than 15 percent, local oscillator power of 0.5 milliwatts or less will be sufficient

- If sensitivity to 1500 MHz is required, the $R_s G_D$ product must be less than 10^{-2}, the quantum efficiency greater than 25 percent, the diode capacitance less than 8 pf, and the local oscillator power requirement from 1 to 2 milliwatts
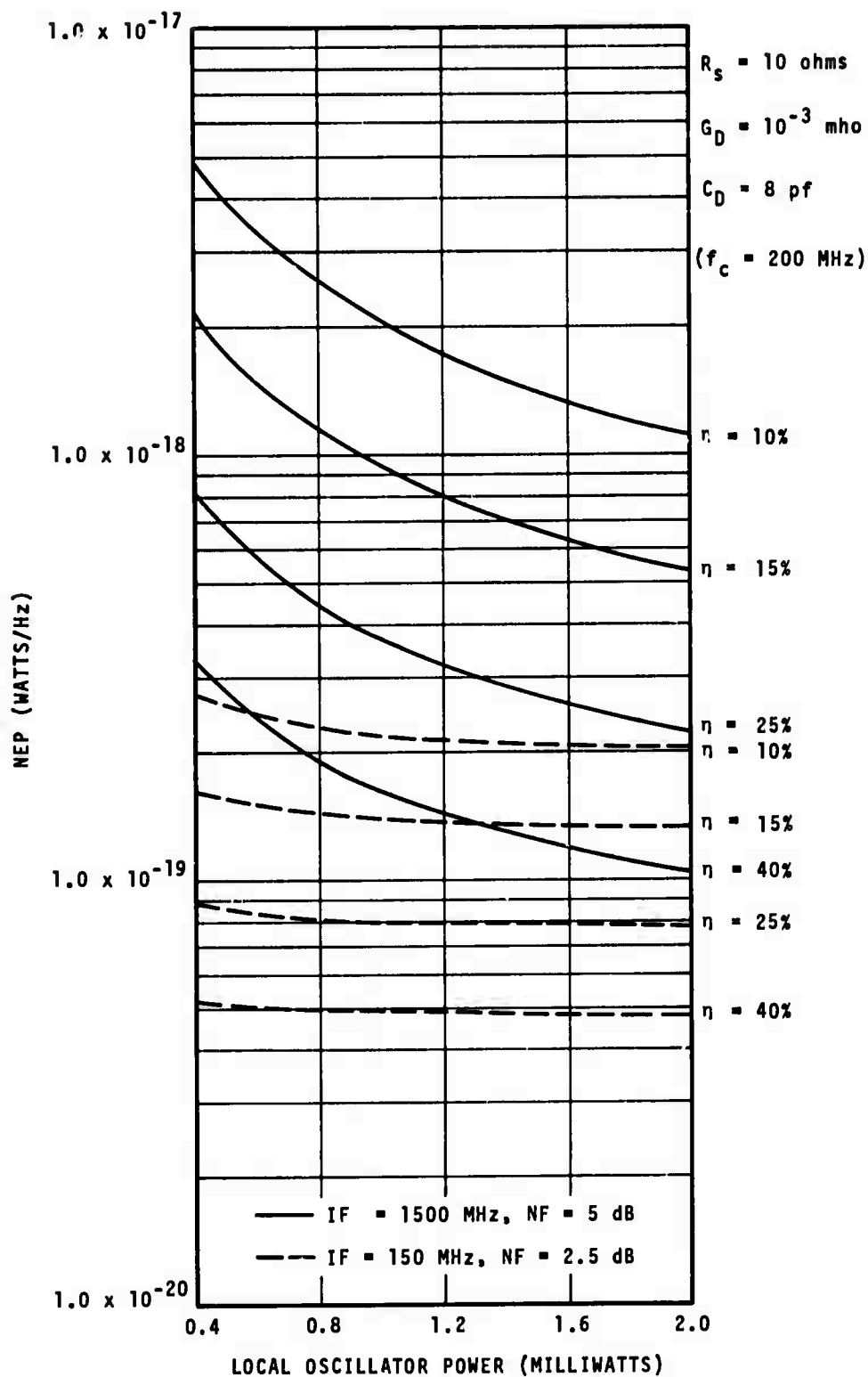
FIGURE 13. NEP VARIATION WITH LOCAL OSCILLATOR POWER VERSUS
QUANTUM EFFICIENCY

2-3965
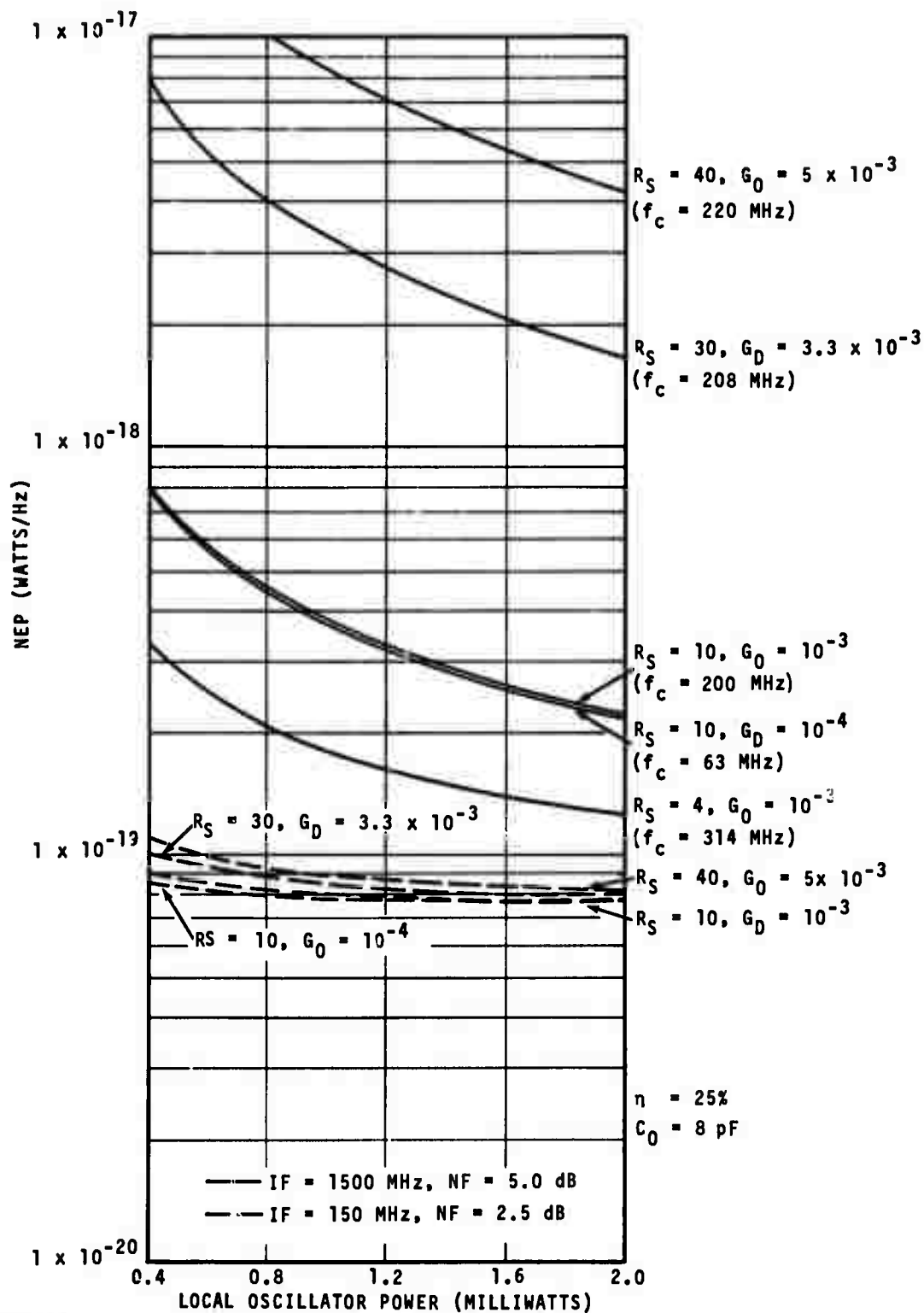
26

FIGURE 14. NEP VARIATION WITH LOCAL OSCILLATOR POWER VERSUS $(R_S \cdot G_D)$
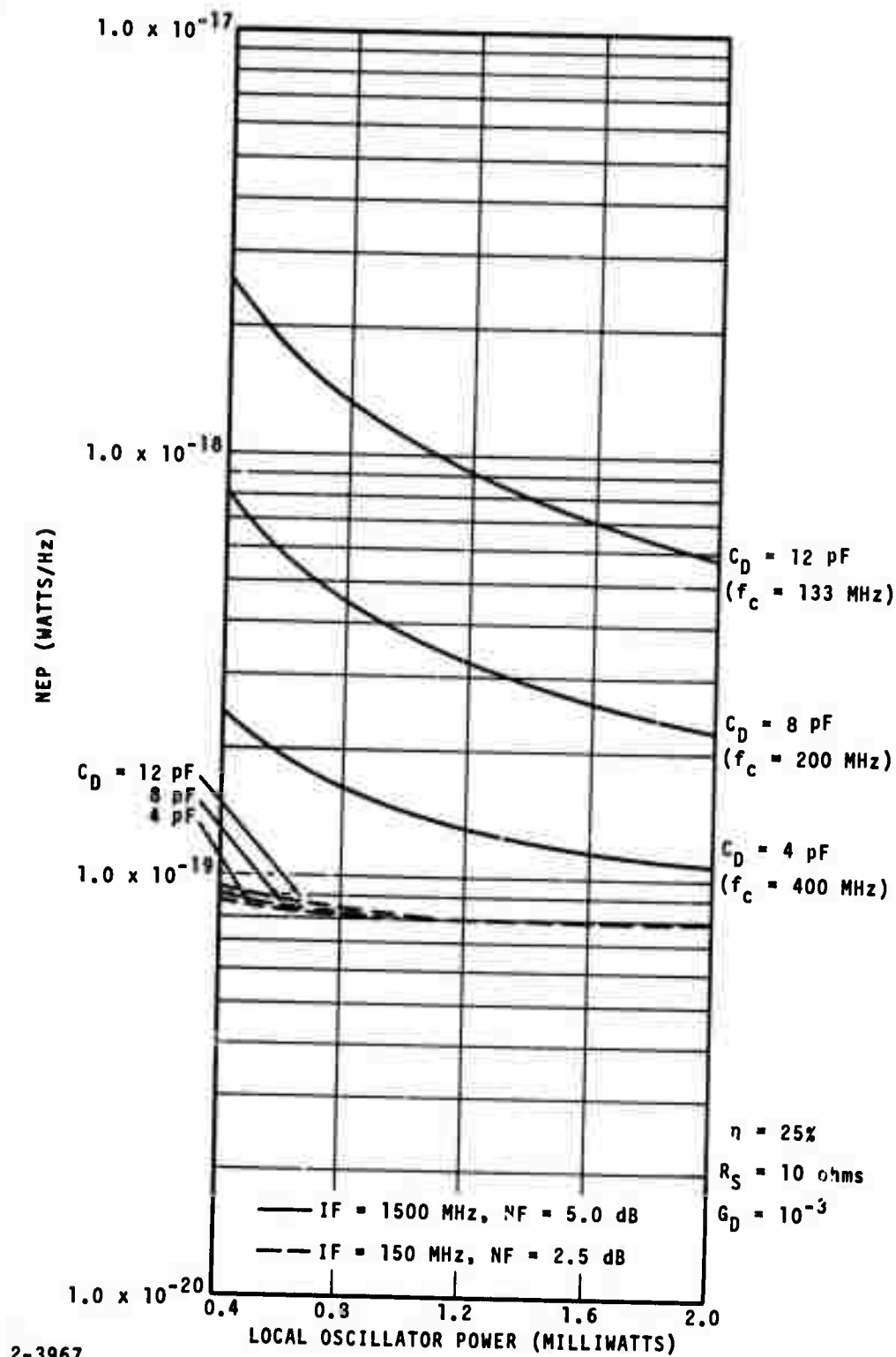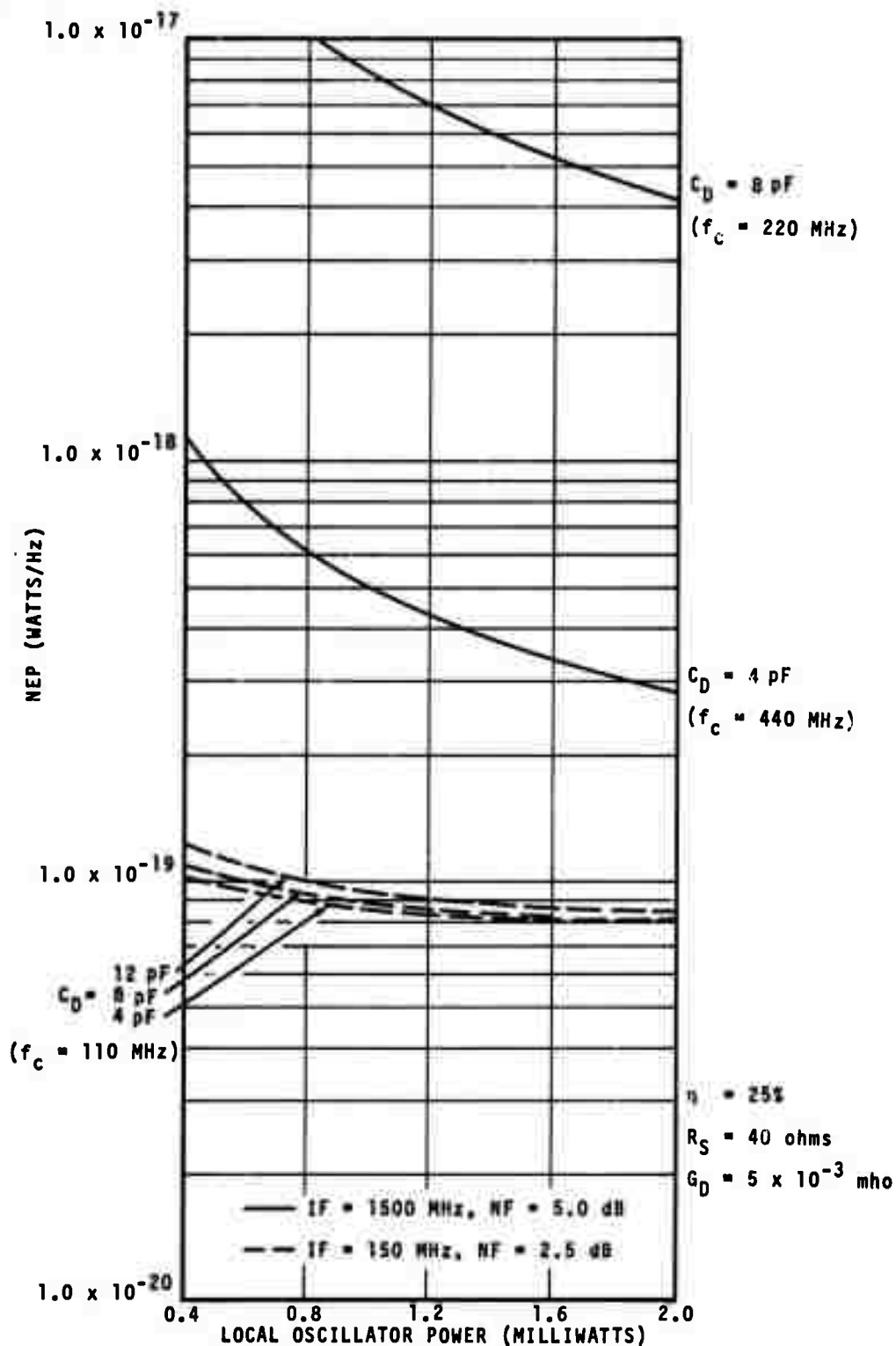
FIGURE 15. NEP VARIATION WITH LOCAL OSCILLATOR POWER VERSUS MIXER CAPACITANCE C_D FOR $R_S G_D = 10^{-2}$

2-3967

FIGURE 16. NEP VARIATION WITH LOCAL OSCILLATOR POWER VERSUS
MIXER CAPACITANCE C_D FOR $R_S G_D = 0.2$

- A high quality diode with good front to back ratio ($R_s G_D \ll 1$) will have good sensitivity well beyond its cutoff frequency providing $G_D < 10^{-3}$ has because the mixer available conversion gain G is inversely proportional to G_D.

$$G \approx \frac{C}{G_D} \cdot \frac{1}{1 + \left(\dfrac{f}{f_c}\right)^2} \tag{13}$$

B.   DC BIAS POWER

The dc bias power dissipated in the mixer is the sum of the power due to the diode leakage current and the photo-induced current produced by the local oscillator. The leakage current of present high speed photodiodes with high reverse resistance may be 10-20 percent as large as the photo-induced current when the diodes are biased below the current breakdown region and local oscillator powers on the order of 0.5 to 2 milliwatts are used. From this we can deduce that for a first order calculation of the heat load imposed by a HgCdTe photodiode on a cooler, we can neglect the dc bias power since its major component comes from the local oscillator power which is converted to electrons in the photodiode.

C.   100-ELEMENT ARRAY POWER DISSIPATION REQUIREMENTS

The total power dissipation requirements of the 10 × 10 array of photomixers can now be determined. From the array optical design and Figure 2, we see that for a single element of the array, the local oscillator focused spot, and the first ring of its diffraction pattern fall entirely upon the photosensitive surface of the mixer. In this case, more than 90 percent of the local oscillator power falls upon the mixer and must be absorbed by the mixer and dissipated by the array cooler. This assumes that the reflected and scattered power from the front surface of the mixer is dissipated by other portions of the cooler. Then the maximum total dissipation is 2 milliwatts per element and for the 100 element array the maximum total power dissipated by the mixers is estimated to be 200 milliwatts.

IV. PLAN FOR NEXT QUARTER

- High density cabling techniques will be examined and a breadboard will be constructed using the selected technique

- A thermal analysis will be performed for 4.2 K Ge:Cu photoconductive mixer elements with frequency responses of 150 and 1500 MHz for a 10×10 matrix array

- A thermal mockup of a 77 K, 1.5 GHz, 10×10 array will be constructed and tested